Hydrogenation of Glucose to Sorbitol over Nickel and Ruthenium Catalysts

Burkhard Kusserow, Sabine Schimpf, Peter Claus*

Ernst-Berl-Institute of Chemical Engineering and Macromolecular Chemistry, Darmstadt University of Technology, Petersenstr. 20, 64287 Darmstadt, Germany
Fax: (+49)-6151-16-5369, e-mail: claus@ct.chemie.tu-darmstadt.de

Received: August 2, 2002; Accepted: October 27, 2002

Abstract: Hydrogenation of aqueous glucose solution was performed in batch and continuous reactors using supported nickel and ruthenium catalysts. Preparation methods were precipitation, impregnation, sol-gel and template syntheses, and SiO_2, TiO_2, Al_2O_3 and carbon were used as support materials. A procedure for the one-step synthesis of templated metal on support catalysts was established. The influence of support material and preparation methods was studied and the results were compared with those of an industrial nickel catalyst. In a detailed study taking more than 1100 h time on stream we investigated the deactivation of the industrial catalyst and a supported ruthenium catalyst, and evaluated the deactivation mechanisms. As yet unpublished side products of the glucose hydrogenation were identified and a scheme of the reaction network was set up.

Keywords: deactivation; glucose hydrogenation; leaching; mesoporous molecular sieves; nickel catalyst; ruthenium catalyst

Introduction

Sorbitol is the polyol with the most widespread use in nutrition, cosmetics, medical and industrial applications. It is used as a low calorie sweetener and sugar substitute for diabetics, as a humectand in cosmetic and pharmaceutical products, in paper and tobacco and other applications. It has no cariogenic activity, so most toothpastes are based on sorbitol. Additionally, sorbitol does not undergo the Maillard reaction. It is used as a feedstock for vitamin C and for diol components for the production of polymers. The world-wide production volume exceeded 1,000,000 tons/a in 2000.

Sorbitol is produced by catalytic hydrogenation of aqueous glucose solutions with glucose contents of up to 65 wt %, either in discontinuous (autoclave) or continuous (trickle bed) reactors under high pressure.

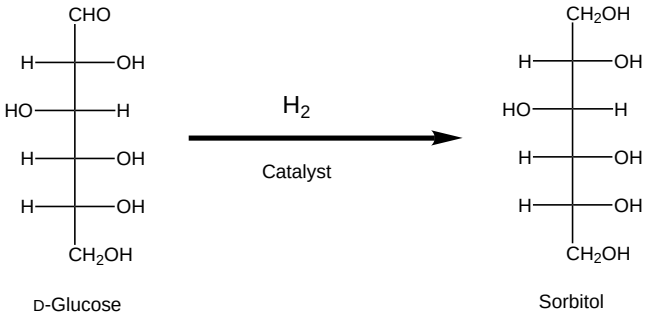

Figure 1. Hydrogenation of glucose to sorbitol.

Up to now, most catalysts for sorbitol hydrogenation are based on nickel as active metal. Historically, Raney nickel was used because of its economic price, later supported nickel catalysts were more frequently used because they are more active. To increase activity some investigators used promoted nickel catalysts. Li et al.[1] used nickel-boron amorphous alloy catalysts promoted with chromium, molybdenum and tungsten and found highest activities for catalysts promoted with tungsten. In another article, Li et al.[2] used Raney nickel promoted with phosphorus. Gallezot et al.[3] studied Raney nickel promoted with molybdenum, chromium, iron and tin. The kinetics of the continuous glucose hydrogenation with a supported nickel catalyst in a trickle bed reactor was studied by Déchamp et al.[4] But nickel has some disadvantages: the nickel leaches, resulting in a loss of activity and a high nickel content in the sorbitol solution. For use in food, medical and cosmetic applications, the nickel must be removed completely from the sorbitol, resulting in high additional costs. Therefore, catalysts based on other active metals were evaluated, including cobalt, platinum, palladium, rhodium and ruthenium.[1,5,6] The best activities were found for supported ruthenium catalysts. Furthermore, ruthenium is not dissolved under the reaction conditions of the glucose hydrogenation.[5,6] K. van Gorp et al.[7] used ruthenium on carbon supports for discontinuous hydrogenation of glucose, Heinen et al.[8]

  1615-4150/03/3451+2-289–299 $ 17.50+.50/0

used the same combination for the hydrogenation of fructose to mannitol.

Continuous hydrogenation of glucose with ruthenium catalysts in a trickle bed reactor was performed by Arena[9] and Gallezot et al.[10] Arena focused his interest on the deactivation mechanisms of catalysts composed of ruthenium on alumina supports. He found physical changes in the support material and poisoning by gluconic acid, iron and sulphur as causes for deactivation. Gallezot used ruthenium on carbon supports. A catalyst with a ruthenium load of 1.6 wt % had a conversion rate of 98.6% after 52 – 69 h time on stream (TOS), the conversion rate dropped to 94.4% after 312 h TOS, indicating a remarkable deactivation of the catalyst.

The aim of our study was to overcome the deactivation and leaching problems associated with the present commercial nickel catalysts. One way was to change support materials and preparation methods to achieve a better anchoring of the nickel crystallites on the support. This was tried by sol-gel and template methods for the preparation of the catalysts. Additionally, we investigated impregnation methods using a complexing agent (ethylenediamine) for nickel on various supports.

The other method was the exchange of the active metal. Ruthenium, already known as a very active catalyst metal for glucose hydrogenation, was used on different supports. Preparation was done by precipitation and impregnation. We additionally prepared a ruthenium template catalyst. The catalysts were tested in an autoclave, the best ruthenium catalyst was used for a deactivation study in a trickle bed reactor for 1155 h TOS.

The characterisation of the catalysts was done by the following techniques: atomic emission spectroscopy (ICP-OES) to estimate the metal contents of the catalysts, temperature programmed reduction or oxidation (TPR/TPO), transmission electron microscopy (TEM) to determine the metal particle size as well as X-ray photoelectron spectroscopy (XPS). H_2 chemisorption was used to estimate the metal surface of some catalysts. ICP-OES was also used to investigate the metal leaching by determining the metal content in the product solution. The elemental composition of one catalyst was analysed with X-ray fluorescence (XRF).

Results and Discussion

Reaction Network

The hydrogenation of glucose produced some by-products. Our experiments yielded up to 8 wt % of these compounds. The highest amounts of by-products (~8 wt %) were produced by supports based on TiO_2, followed by supports based on Al_2O_3 (5.5 – 7.5 wt %) and carbon (3.4 – 6.3 wt %). Supports based on SiO_2

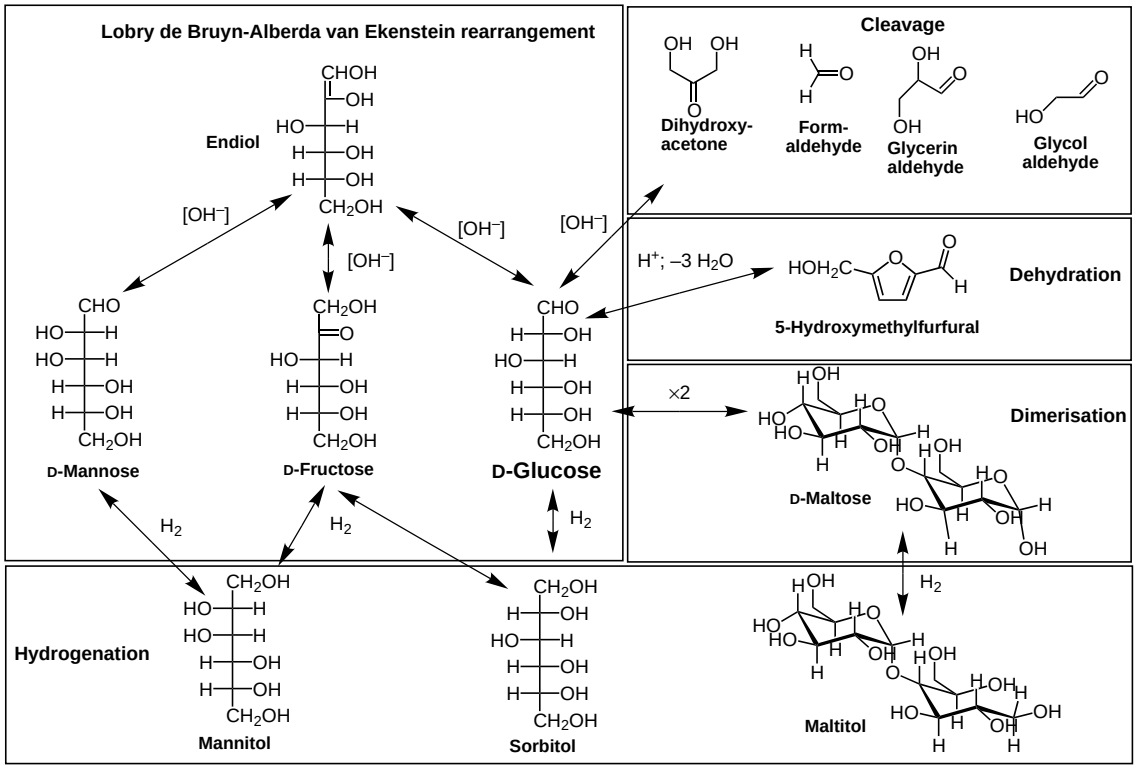

Figure 2. Reaction network for the hydrogenation of glucose.

produced less by-products (2.1 – 4.1 wt %). Most of these by-products had been unknown so far. As sorbitol is used for nutrition and as some of the by-products were responsible for deactivation of the catalysts,[9] it is important to identify these compounds. We investigated these products by comparison with standards, after derivatisation with hydroxylamine (both HPLC) and with GC subsequent to the derivatisation with hexamethyldisilazane. We identified mannose, fructose, maltose, glycerin aldehyde, dihydroxyacetone, glycol aldehyde, formaldehyde, 5-hydroxymethylfurfural, mannitol, maltitol and iditol. From these, fructose, mannitol and iditol were already reported by other research groups.

The primary by-products were built by non-catalytic pathways. Mannose and fructose were products of the Lobry de Bruyn – Alberda van Ekenstein rearrangement, glycerin aldehyde, dihydroxyacetone, glycol aldehyde, formaldehyde were formed by alkaline cleavage of sugars and 5-hydroxymethylfurfural was formed by dehydration. 5-Hydroxymethylfurfural is a marker substance for non-enzymatic browning under acidic conditions in absence of amines.[11] In our experiments, 5-hydroxymethylfurfural was detectable before a yellow colour of the product solution occurred, indicating its usefulness as a marker. It seems to be surprising that alkaline cleavage of sugars could take place at a pH of 3 – 4, depending on the experiment. We consider the alkaline properties of the surface of the support as source for this reaction. Acidic properties of supports may also be the reason for the formation of 5-hydroxymethylfurfural. No experiment yielded both products of the alkaline decay and 5-hydroxymethylfurfural at once. This conjecture is supported by the observation that these compounds were also produced by the pure supports of the corresponding catalysts. In blank runs we found fructose, mannose and maltose in small quantities (< 2 wt %) but products of the cleavage and 5-hydroxymethylfurfural were not found. The hydrogenation products of these compounds were mannitol and maltitol. Hydrogenation products of the other carbonyls were not found, probably because they react slower than glucose. Heinen et al.[8] reported that glucose adsorbs much stronger on Ru-catalysts than fructose, leading to an inhibition of the hydrogenation of fructose under mild reaction conditions. According to this, the mannitol yield is low compared to fructose even when glucose conversion to sorbitol is high in our experiments. This may also be a limiting factor for the hydrogenation of the other by-products.

The formation of iditol is not yet explained. In the literature, the common explanation is isomerisation of sorbitol. But it still cannot be explained why iditol should be the only product of the isomerisation. Some minor by-products remained unidentified. The identification of most of these compounds allows the formulation of a reaction network, see Figure 2.

Characterisation and Catalytic Results of the Nickel Catalysts Prepared with Ethylenediamine

The catalysts were prepared by impregnation (marked by the suffix "en") and incipient wetness (marked with the suffix "Ren") with aqueous solutions of [Ni(ethylenediamine)$_n$(H_2O)$_{6-2n}$](NO_3)$_2$. The catalysts, the supports, the formation method used and the metal contents are displayed in Table 1. All catalysts were characterised by their reaction results, metal contents and by the analysis of the product solution for nickel leaching. Reactions were performed with 50 wt % glucose solution in an autoclave at 393 K, 0.5 g of catalyst and at a hydrogen pressure of 120 bar. Selected catalysts were further investigated with XRD for nickel crystallite sizes, with TPR and chemisorption.

Table 1. Nickel catalysts prepared via ethylenediamine, catalyst name, support, thermal treatment, Ni content of the catalyst and of the product solution after the reaction.

Catalyst	Support	Thermal treatment[b]	Nickel content [wt %]	Leaching [μg × ml^{-1}]
Ni68T[a]	SiO_2		66.78	125.87
Ni/Al_2O_3 C-en	Al_2O_3 C	A	5.07	66.32
Ni/Al_2O_3 C-Ren	Al_2O_3 C	A	9.11	68.77
Ni/TiO_2-en	TiO_2 P25	A	3.26	22.29
Ni/TiO_2-Ren	TiO_2 P25	A	6.87	30.61
Ni/SiO_2 F10-en	Silica gel large pore 58 micron	A	16.92	79.94
Ni/SiO_2 F10-Ren	Silica gel large pore 58 micron	A	12.93	100.23
Ni/SiO_2 F11-en	Silica gel large pore 99.5%	A	5.48	40.47
Ni/SiO_2 F11-Ren	Silica gel large pore 99.5%	A	12.83	34.10
Ni/C(I)-en	Black Pearls 2000 GP3755	B	4.81	1.61
Ni/C(I)-Ren	Black Pearls 2000 GP3755	B	5.55	7.04
Ni/C(II)-en	Vulkan XC72R GP3759	B	5.62	6.11

[a] Industrial nickel catalyst for comparison.
[b] A: calcinated in air at 773 K, reduced in H_2 at 773 K; B: heated in He at 623 K, reduced in H_2 at 773 K.

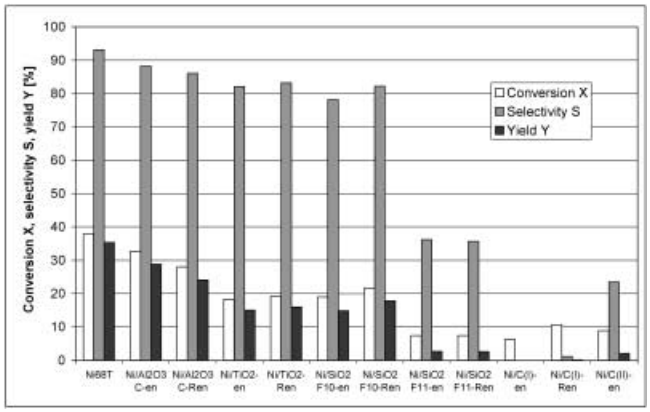

Figure 3. Conversion of glucose, selectivity and yield to sorbitol of the nickel catalysts prepared with ethylenediamine, discontinuous hydrogenation.

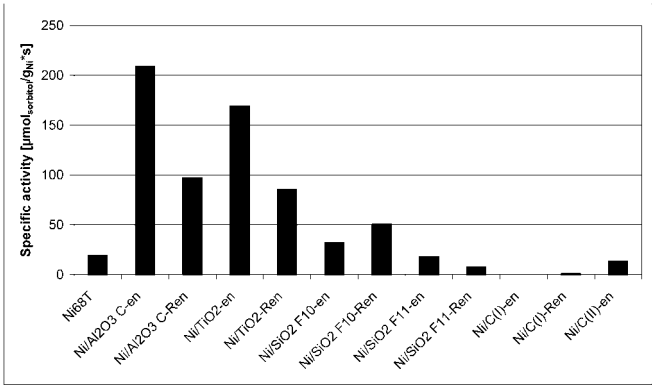

Figure 4. Specific activity of the catalysts prepared with ethylenediamine, discontinuous hydrogenation.

Table 2. Nickel crystallite sizes for selected catalysts prepared with ethylenediamine.

Catalyst	Ni particle size [nm]
Ni/Al_2O_3 C-en	2.2
Ni/Al_2O_3 C-Ren	4.7
Ni/TiO_2-en	9.7
Ni/SiO_2 F10-en	2.5/10.2
Ni/SiO_2 F10-Ren	2.6/11.6

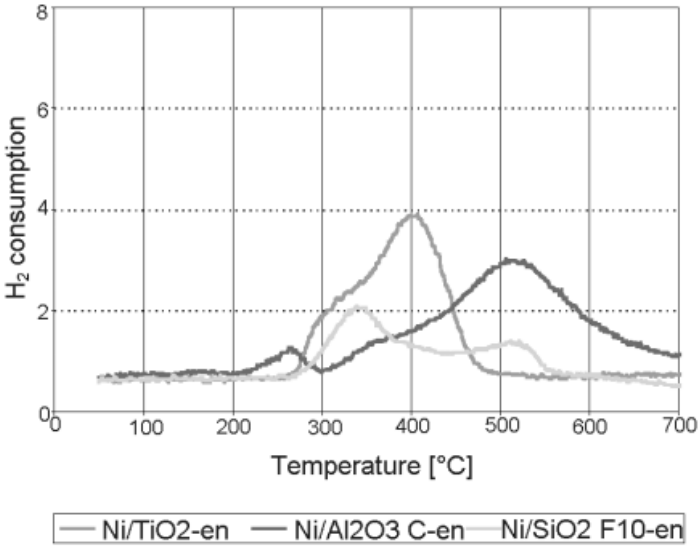

Figure 5. Temperature programmed reduction of selected catalysts prepared with ethylenediamine.

At the beginning, we used different reduction temperatures for these investigations. Since catalysts reduced at 773 K had a higher activity than those reduced at 573 K, we used the higher reduction temperature for further investigations.

Regarding the catalytic results, displayed in Figure 3, alumina seems to be the best support for catalyst preparation. Ni/Al_2O_3 C-en shows conversion comparable with the industrial catalyst, but the selectivity to sorbitol is only 88%, whereas the industrial catalyst reached 92% selectivity at same conditions. The catalysts prepared on titania and silica had lower conversion, the carbon supports used were not suited for this reaction. Regarding the specific activities of the catalysts, expressed as µmol sorbitol per gram nickel and per second, displayed in Figure 4, the activity follows the sequence $Al_2O_3 > TiO_2 > SiO_2 > C$. In most cases, catalysts prepared by impregnation had a higher activity than those prepared by incipient wetness.

Some of these catalysts were also investigated with XRD to estimate the nickel crystallite size, the results are given in Table 2. This demonstrates that the nickel crystallites are smaller for Ni/Al_2O_3 C-en (2.2 nm) than for Ni/Al_2O_3 C-Ren (4.7 nm). This explains the higher activity for the catalyst prepared by impregnation. Ni/TiO_2-en had a high activity in spite of its relatively large crystallite size (9.7 nm). The catalysts Ni/SiO_2 F10-en and Ni/SiO_2 F10-Ren had a bimodal crystallite size distribution with one population of a mean size of approximately 2.5 nm diameter, the other of about 11 nm.

TPR analysis of these catalysts (Figure 5) showed that the reduction temperature depends on the nature of the support. The bimodal crystallite distribution of Ni/SiO_2 F10-Ren is also shown as two maxima at $T = 613$ K and $T = 793$ K in the TPR diagram.

H_2 chemisorption was performed to estimate the Ni surface. For the 5 catalysts shown in Figure 6, Ni surfaces were in the range between 1.3 and 17 $m^2/g_{catalyst}$. Figure 6 shows the Ni surface, the Ni content, the specific activity and overall yield for the catalysts. These results suggest that catalytic results depend on the nature of the support rather than on nickel content or nickel surface of the catalyst. A possible explanation is that the support has an influence on the balance between the tautomeric forms of glucose. Makkee et al.[12] reported for the hydrogenation of fructose over Cu and Ni catalysts that

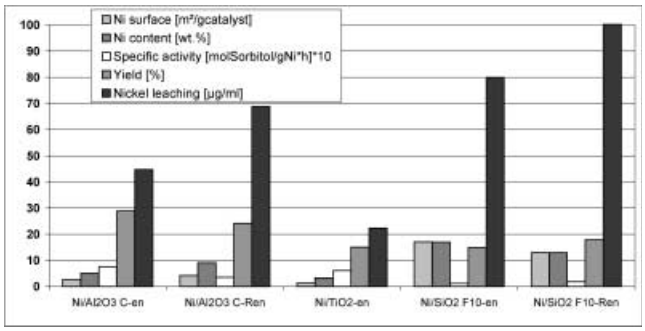

Figure 6. Ni surface, Ni content, specific activity, yield and Ni leaching of selected catalysts.

the different tautomeric forms had different reactivities, so a change of this balance will result in a change of the overall reactivity. Glucose reacts predominantly as the open-chain form, thus a higher concentration of this form will result in higher conversion rates.

All tested catalysts were leaching (see Table 1). Together with the relatively low nickel content of the best catalysts, this will result in a rapid deactivation. For this reason no experiment in the trickle bed reactor was performed.

Characterisation and Catalytic Results of Sol-Gel and Template Catalysts

The discontinuous hydrogenation of glucose was performed with 50 wt % glucose solution in an autoclave at 393 K and at a hydrogen pressure of 120 bar. The sol-gel catalysts gave no conversion to sorbitol. In BET analysis, a BET surface of 350 $m^2\ g^{-1}$ was measured, the BJH pore size was <2 nm. We deduced from this that the pore size was too low for an effective transport of glucose in the pores. Therefore we do not give explicit data on these experiments. So we made the following syntheses using a templating strategy to reach wider pores.

Mesoporous molecular sieves synthesised with surfactants as templates have been investigated since 1992.[13] Despite their use as supports for catalytic active metals, only few applications[14] deal with the direct synthesis of templated metal on support catalysts of this type. We tried to develop generalised procedures for one-step syntheses of templated metal on support catalysts. One of these strategies involved the suspension of an organic metal precursor (e.g., nickel acetylacetonate) in the template solution. The precursor was dissolved in the micelles of the surfactant and the support precipitated after addition of tetraethyl orthosilicate (TEOS) around the micelles. We added different amounts of toluene to the synthesis mixture to influence the pore diameter of the resulting materials. These catalysts were indexed with the suffix Org. The template was removed in the calcination step.

Another strategy is to synthesise templated supports with organic anchor groups which serve as ligands for ions of the active metal. Now we used trimethylsilylpropyl-ethylenediamine as complexing agent. The anchor precursor was added to the TEOS and both were added to the template solution. After precipitation of the support, either a metal salt was added directly to the reaction mixture (Ni20Sp1), or, for use as a stock for different metals on support catalysts, the template was extracted from the support and the metal salt was added to a slurry of the support (Ni20S and Ru2S).

We synthesised catalysts with nickel, ruthenium and silver and used them in different reactions. Here we report only the results in the hydrogenation of glucose.

Characterisation of the catalysts was done with N_2 physisorption and by analysis of the nickel content of the catalyst and the product solution. The results are displayed in Table 3.

All template catalysts showed a very narrow pore size distribution, BET surfaces ranged from 366 to 803 $m^2\ g^{-1}$. For the series of Org-catalysts, we expected an increase in pore diameter with increasing toluene concentration. Surprisingly, we registered the opposite. A competition between the nickel acetylacetonate and the toluene on the place in the micelles of the template can explain this behaviour; accordingly, we found a decrease of nickel content in the resulting catalyst with increasing toluene content in the synthesis mixture.

There is a strong correlation between toluene concentration and pore diameter for these catalysts, represented in Figure 7. This now enables us to synthesise catalysts with predefined pore sizes.

Nickel leaching was estimated by analysis of the product solution for the catalysts Ni20Org1 and Ni20Sp1, the results were 87.26 and 32.74 µg nickel ml^{-1} product solution, respectively. This indicates a relatively high leaching for both catalysts. In Figure 8,

Table 3. Properties of the template catalysts.

Catalyst	Ni20Org1	Ni20Org2	Ni20Org3	Ni20Sp1	Ni20S	Ru2S
BET [$m^2\ g^{-1}$]	367	803	708	464	604	509
BJH[a] Pore size [nm]	5.5	4.3	3.3	5.1	1.5	1.5
Metal content [wt %]	21.4	18.5	10.4	20.3	2.1	2.0
Sorbitol yield [%]	7.7	4.2	6.8	2.9	0.5	4.1

[a]Pore size calculation method from Barret, Joyner and Halenda.

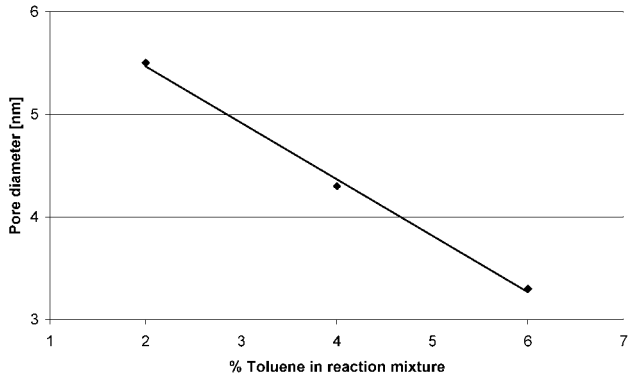

Figure 7. Dependence of the pore diameter from the toluene content of the synthesis mixture for the catalysts Ni20Org1, Ni20Org2 and Ni20Org3.

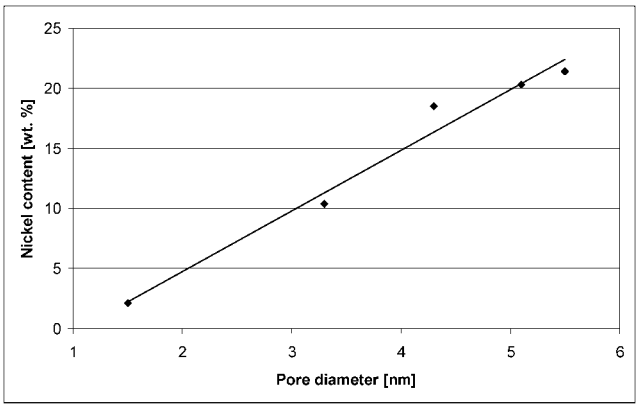

Figure 8. Dependence of the nickel content from the pore diameter for the templated nickel catalysts.

the correlation between pore diameter and nickel content of all template catalysts is shown.

Glucose hydrogenation results, displayed in Table 3, are insufficient for all template catalysts compared to the industrial catalyst, which exhibited a sorbitol yield of 35%. Also, most catalysts prepared with ethylenediamine yield more sorbitol (up to 29 wt %). Ni20Org1, with the highest nickel content and the widest pores yielded most sorbitol (7.7%), Ni20S with the lowest nickel content and the narrowest pores gave least sorbitol (0.5%). We think that the low overall conversion is caused by a transport limitation in the long and relatively narrow pores of these materials. This is supported by high conversion rates for these catalysts in the hydrogenation of smaller molecules (e.g., acrolein and citral). Ni20Sp1 showed a different behaviour, in spite of its high nickel content and pore diameter, the sorbitol yield was very low. The present data are inadequate for an explanation. Insufficient reduction of the catalyst may be the reason, however. The reduced catalyst was grey, Ni20Org1 with comparable nickel content and pore diameter was black. The higher sorbitol yield of Ru2S (4%) compared to Ni20S (0.5%) reflected the higher activity of ruthenium compared to nickel. Taking into account the low conversion rate and the relatively high leaching of nickel, these catalysts were not suited for the hydrogenation of glucose.

Characterisation and Catalytic Results of the Ruthenium Catalysts

Because of the high activity of ruthenium compared to nickel, the ruthenium catalysts were prepared with lower metal contents than the nickel catalysts. Metal contents for the Ru catalysts were between 0.1 and 2.8 wt %. The catalysts are listed in Table 4, preparation methods and supports are also given. In Figure 9 the catalytic results are displayed.

The discontinuous hydrogenation of glucose was performed with 50 wt % glucose solution in a autoclave at 393 K and at a hydrogen pressure of 120 bar. Ruthenium catalysts with 1 wt % or more ruthenium had conversion rates equal or superior to the commercial catalyst Ni68T. The selectivities were slightly lower, caused by the formation of side products. The produc-

Table 4. Catalyst name, preparation method, support, metal content and metal particle size of the ruthenium catalysts.

Catalyst	Preparation method	Support	Metal content [%]	Particle size [nm]
Ru3Ap	precipitation	Al_2O_3 C	2.75	1.0
Ru1Ap	precipitation	Al_2O_3 C	1.04	1.4
Ru1Ai	impregnation	Al_2O_3 C	0.95	1.6
Ru09Ai	impregnation	Al_2O_3	0.97	1.9
Ru08Ai	impregnation	Al_2O_3	0.84	–[b]
Ru05Ai	impregnation	Al_2O_3	0.47	1.8
Ru03Ti	impregnation	TiO_2 P25	0.27	–
Ru01Ti	impregnation	TiO_2 P25	0.11	–
Ru1Ti	impregnation	TiO_2	1.01	–
Ni68T[a]	precipitation	SiO_2	66.78	–

[a] Industrial nickel catalyst for comparison.
[b] Not measured.

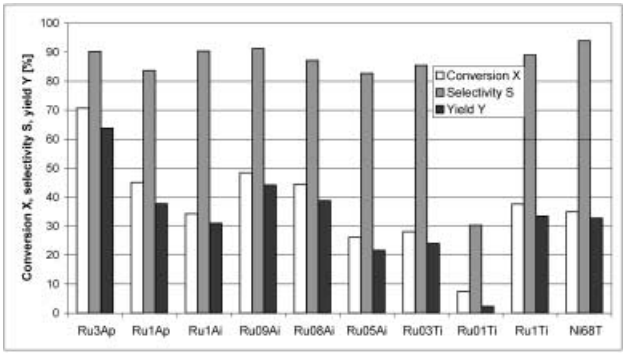

Figure 9. Conversion of glucose, selectivity and yield to sorbitol of the ruthenium catalysts compared with the industrial nickel catalyst Ni68T.

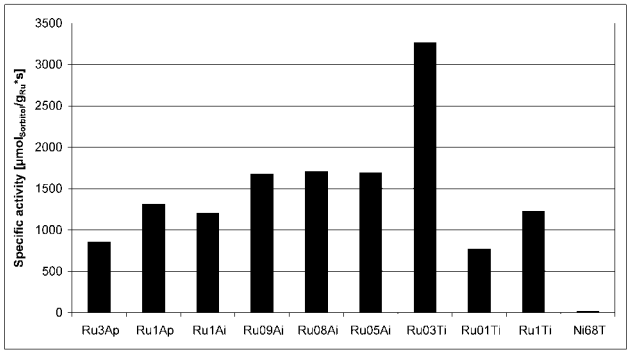

Figure 10. Specific activity, given as µmol sorbitol per gram catalyst and hour of the ruthenium catalysts compared with the industrial nickel catalyst Ni68T.

tion of side products depended on the support and the contact time. In experiments performed in the trickle bed reactor we found smaller amounts of side products. The specific activity of the catalysts, shown in Figure 10, is highest for ruthenium contents between 0.3 and 0.9 wt %, catalysts with higher or lower ruthenium contents displayed lower specific activities.

We could not detect any leaching of ruthenium in our experiments, ruthenium detection limit was 80 µg L^{-1} of product solution.

These results were promising, so a larger quantity of a ruthenium catalyst was prepared on a alumina support and used for a long-time experiment in the trickle bed reactor.

Continuous Hydrogenation

We investigated the commercial comparison catalyst Ni68T and the ruthenium catalyst Ru05Ai for more than 1100 h time on stream (TOS) in the trickle bed reactor under standard conditions: 40 wt % glucose solution was delivered at a flow rate of 40 mL/h to the reactor packed with 40 mL of catalyst, H_2 flow was 23 L/h at a

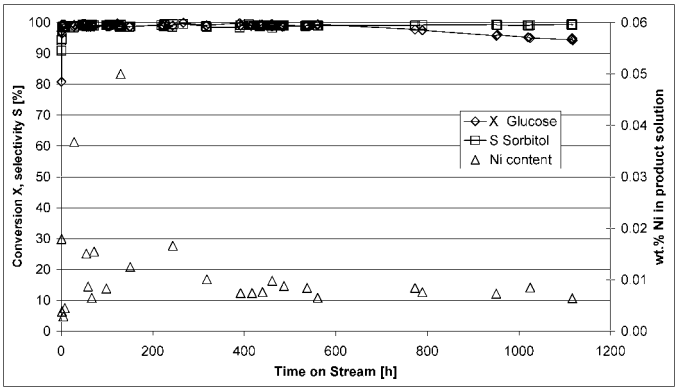

Figure 11. Conversion of glucose, selectivity to sorbitol and nickel leaching of the industrial catalyst Ni68T during more than 1100 hours time on stream in continuous hydrogenation.

pressure of 80 bar, reaction temperature was 353 K. The results are represented in Figure 11 for the nickel catalyst and will be given later for the ruthenium catalyst. At the beginning of the experiment, the conversion of glucose was 99.3% for the nickel catalyst and 99.9% for the ruthenium catalyst. Selectivity to sorbitol was 98.8% and 99.0%, respectively. The conversion dropped below 98% after 770 h TOS for the nickel catalyst, after 1080 h TOS for the ruthenium catalyst. The selectivity for both catalysts remained unchanged during the experiments.

Deactivation

After 250 h TOS the commercial nickel catalyst showed a nearly constant level of leaching over the whole reaction time (see Figure 11). Higher leaching at the beginning of the experiment was probably due to the loss of small particles of the catalyst remaining after the initial rinsing step. In TEM pictures of the fresh and the used catalyst, see Figures 12 and 13, we registered a change in particle size distribution to higher crystallite sizes resulting in a loss of active surface after 400 h TOS.

The particle size distribution changed from a monomodal to a bimodal distribution. The particles sized between 1 – 9 nm had completely disappeared, particles with a diameter >10 nm had been built up. In XRD analysis, the mean particle size increased from 10 nm to 29 nm. The nickel content of the catalyst decreased by 25% (from 66.78 wt % to 50.53 wt %) during the experiment. There appeared also a visible disintegration of the support, not surprising for silica under hydrothermal conditions. The BET surface decreased by 60% (from 180 to 85 m^2 g^{-1}) during this time. Additionally, the pore size distribution changed considerably. We registered an increase in the fraction of mesopores, the fraction of micropores decreased. Therefore the stability problems were caused by the hot and acidic reaction media (pH 4

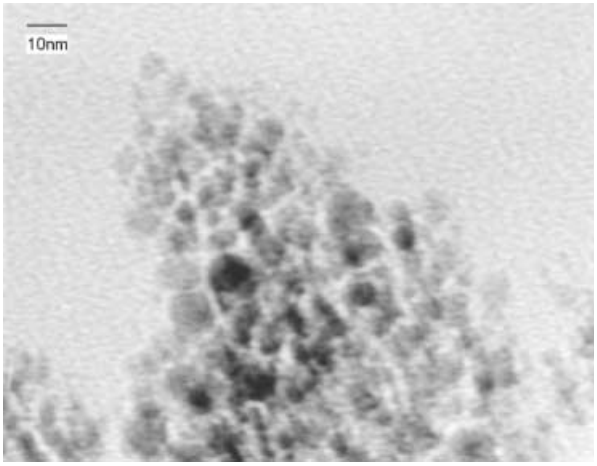

Figure 12. TEM image of the unused industrial catalyst Ni68T.

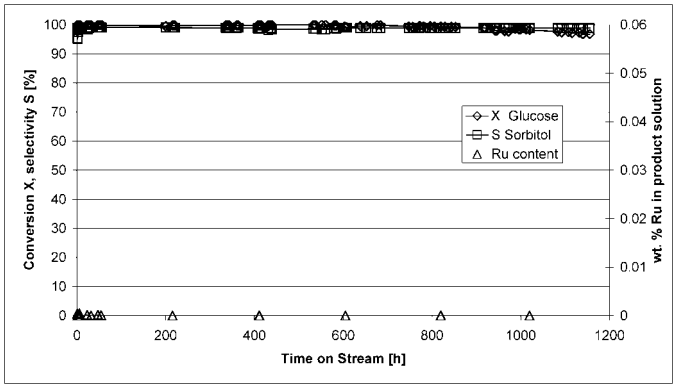

Figure 14. Conversion of glucose, selectivity to sorbitol and ruthenium leaching of the catalyst Ru05Ai during 1150 h TOS in continuous hydrogenation.

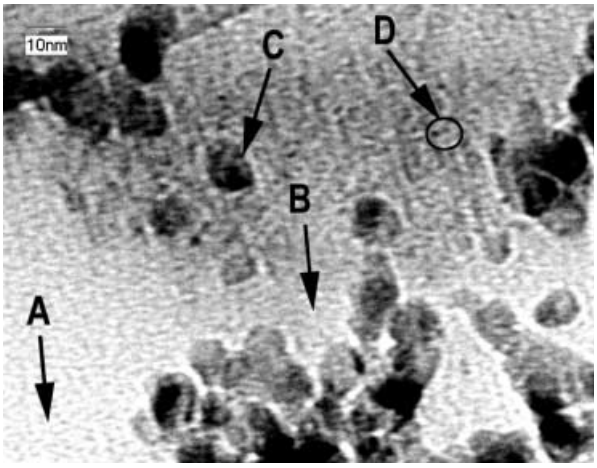

Figure 13. TEM image of the industrial catalyst Ni68T after 400 h TOS. A: carbon film, B: SiO_2, C: nickel crystallites >10 nm, D: nickel crystallites about 1 nm.

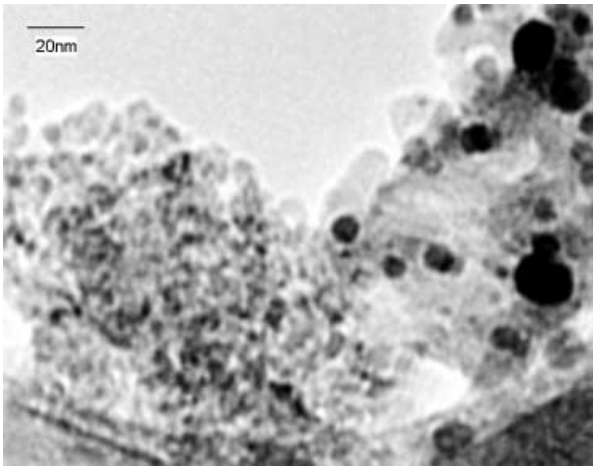

Figure 15. TEM image of the catalyst Ru05Ai after use in the continuous hydrogenation of glucose for 1155 h TOS.

in the product solution). Furthermore glucose and sorbitol are chelating molecules. The result was a permanent drag-out of nickel and silica with the product solution.

The ruthenium catalyst was investigated for 1155 h TOS. The results are displayed in Figure 14. As mentioned above, the conversion of glucose dropped from the initial 99.9% below 98% after 1080 h TOS whereas the selectivity remained unchanged. No leaching of ruthenium could be detected by ICP-OES for Ru05Ai (see Figure 14). BET surface and pore size distribution remained unchanged during this time, XRF spectra of the fresh and the used catalyst indicated no difference in ruthenium content.

The TEM image (see Figure 15) of the used catalyst shows that most of the ruthenium is present in the form of crystallites with diameters below 5 nm. Some crystallites are bigger, in a detailed evaluation we found crystallites up to a diameter of 75 nm. The crystallite size distribution, shown in Figure 16, is monomodal with a maximum at 3 – 4 nm. Within the analytical tolerance we found no difference in particle size distribution between fresh and used catalyst.

Despite this, there is some deactivation after approximately 900 h TOS. After 1155 h TOS we tried to restore the activity by rinsing with distilled water for 72 h under standard conditions to remove possible water-soluble contaminants. The activity decreased further over the rinsing step. A possible reason could be fouling due to high molecular products of the non-enzymatic browning, but we did not find the typical marker substance 5-hydroxymethylfurfural in the product solutions of this experiments. Furthermore, the activity should increase or remain constant over the rinsing step because no further contamination by products of the reaction is possible. Arena[9] identified gluconic acid, iron (from the stainless steel reactor) and sulphur as deactivating compounds. We excluded oxygen by degassing of the

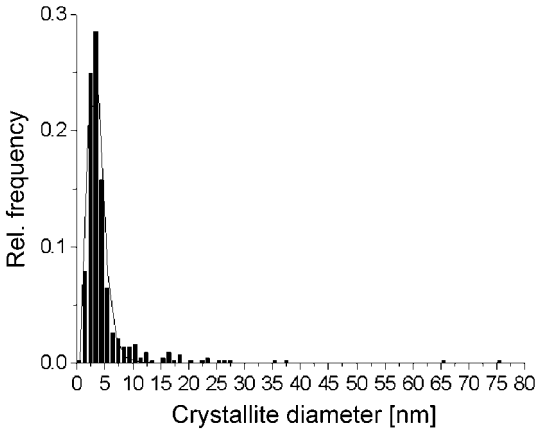

Figure 16. Crystallite size distribution of the catalyst Ru05Ai after use in the continuous hydrogenation of glucose for 1155 h TOS.

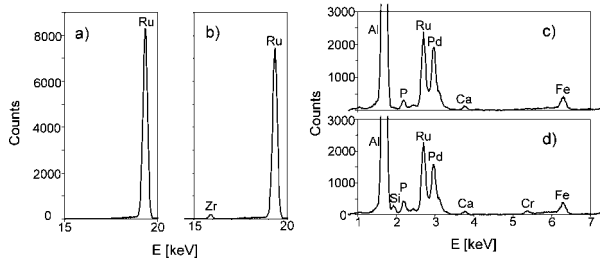

Figure 17. Parts of the XRF spectra showing the elemental composition of Ru05Ai before and after reaction. Picture **a**) before reaction, **b**) after reaction, both with corundum target, **c**) before reaction, **d**) after reaction, both with HOPG target.

feed and storage under helium, in the absence of oxygen there should be no reaction to gluconic acid. Nevertheless we analysed some samples of the product solution for gluconic acid. No gluconic acid could be detected. The sulphur content claimed by the manufacturer of the used glucose is $\leq 0.005\%$, expressed as SO_4^{2-}.

We used XRF to detect changes in the elemental composition of the catalyst. The resulting spectra are shown in Figure 17. We found no sulphur, the iron content of the catalyst remained unchanged during 1155 h TOS. Instead, we found an increase in the content of chromium, silicon and zirconium. Variations for the other elements were within the analytical uncertainty. The standard deviation of the XRF was 2.2% of the peak area (6 experiments). The material of the reactor and tubing was stainless steel 316. This could explain the content of chromium and silicon, but zirconium is not used in SS316. It is also remarkable that some palladium is present in the catalyst, probably because of impurities in the delivered ruthenium acetylacetonate. Whether this had a positive or a negative influence on the catalytic results, is unknown so far.

Therefore we concluded that poisoning by metal impurities, leaching out of the working material of the reactor, is the main deactivation mechanism for the ruthenium catalyst. Teflon liners in the reactor should prevent the poisoning of the catalyst.

Another charge of this catalyst was tested in an industrial pilot plant with a catalyst load of 575 mL over 890 h TOS. The 40 wt % glucose solution was delivered at a flow rate of 0.5 L h^{-1}, reaction temperatures were between 353 K and 393 K, pressure was 24 MPa. Although the reaction conditions were different our results were confirmed.

The catalyst behaves differently in batch and continuous hydrogenation. In batch hydrogenation the catalyst showed a conversion of 26% and a selectivity to sorbitol of 83% compared to the industrial nickel Ni68T catalyst with 41% and 92%, respectively. In continuous reaction, the results with respect to conversion and selectivity were nearly the same for Ru05Ai and Ni68T. These results were confirmed by the industrial application of these catalysts.

Conclusions

Nickel catalysts were deactivated in glucose hydrogenation by leaching of the metal, by changes in the crystallite size distribution and by degradation of the support. A high nickel content is obviously necessary for high activity and long working life. The leaching of nickel in the acidic and chelating reaction media could not be prevented by the preparation methods used here.

Ruthenium catalysts are superior to nickel catalysts in terms of specific activity and lifetime. Conversion of glucose and selectivity to sorbitol were comparable at ruthenium loads of 1% of the nickel content of a commercial nickel catalyst with 66.78 wt % nickel. Furthermore, no ruthenium leaching could be detected. The higher costs of the metal are reduced by a much lower metal content and minor downtime due to the prolonged lifetime of the catalyst. The main deactivation mechanism for the ruthenium catalyst was the poisoning by metals leached out from the reactor material.

In autoclaves a higher ruthenium load of the catalyst is needed to reach catalytic results comparable with industrial nickel catalysts, compared to continuous reactors.

The pore structure of the catalyst had a significant influence on the catalytic results. In catalysts with pores width ≤ 5 nm the transport of glucose was significantly hindered.

Experimental Section

Reagents and Supports

$Ni(NO_3)_2$, nickel acetylacetonate, ethylenediamine, tetraethyl orthosilicate, NH_4OH solution and HPLC water were deliv-

ered by Merck, $RuCl_3$, $Ru(NO)(NO_3)_3$, and ruthenium acetylacetonate by Alfa Aesar. Glucose was purchased from Fluka (BioSelect), N-[3-(trimethoxysilyl)propyl]ethylenediamine by Aldrich, Pluronic 64 was a gift from BASF.

The used commercial supports were TiO_2 P25, Al_2O_3 C (Degussa), silica gel large pore 58 micron, silica gel large pore 99.5% (Alfa Aesar), Black Pearls 2000 GP3755, Vulkan XC72R GP3759 (Cabot) and Ai (KataLeuna).

Preparation of Catalysts

The preparation of catalysts using ethylenediamine (en) was done by impregnation using aqueous solution of $[Ni(en)_n(H_2O)_{6-2n}](NO_3)_2]$.[15,16] As support material several commercial oxides, see Table 1, were used. The catalysts supported on oxides were dried at 363 K, afterwards calcinated (773 K), both in flowing air and reduced (773 K) in flowing hydrogen. In Table 1 this procedure is marked as A. The carbon supports were dried as before and treated with flowing helium (623 K) before reduction. This procedure is marked as B.

Three synthesis procedures were used for the template catalysts. The template was in all cases 2% w/w Pluronic 64 in distilled water. Reactions were performed in a thermostatted vessel at 45 °C, equipped with a reflux condenser and a dropping funnel.

Procedure 1: The template solution (150 mL) was thermostatted under stirring. Different amounts of toluene, 2 (the catalyst named Ni20Org1), 4 (Ni20Org2) or 6 mL (Ni20Org3) and nickel(II) acetylacetonate (4.37 g) were added. After 30 min of stirring, tetraethyl orthosilicate (17.3 g) was added dropwise through the dropping funnel. After about 20 min a green precipitation was formed. The mixture was stirred for 24 h, then the precipitate was removed by filtration, washed 4 times with distilled water and dried in air overnight.

Procedure 2: The template solution (100 mL) was stirred at 45 °C. Tetraethyl orthosilicate (13.84 g) and N-[3-(trimethoxysilyl)propyl]ethylenediamine (3.78 g) as an anchor group for the metal salt were mixed and added dropwise to the template solution. The mixture was stirred for 48 h. $Ni(NO_3)_2 \cdot 6\,H_2O$ (4.95 g) was dissolved in distilled water (10 ml) and added dropwise to the mixture. The colour of the precipitate changed to blue. This mixture was stirred overnight, the precipitate was filtered off and washed with 4 portions of water. The resulting catalyst was named Ni20Sp1.

Procedure 3: The synthesis of the precipitate was carried out like procedure 2, but with a 5-fold charge of the reagents. The precipitate was filtered off, dried in air overnight, and extracted with ethanol in a Soxhlet extractor for 8 h. Afterwards the precipitate was dried again overnight. The precipitate (2 g) was suspended in a mixture of distilled water (20 mL) and ethanol (1 mL). The metal salt [1.93 g $Ni(NO_3)_2 \cdot 6\,H_2O$ for the Ni catalyst Ni20S or 0.126 g $Ru(NO)(NO_3)_3$ for the Ru catalyst Ru2S] was dissolved in distilled water (20 mL) and added to the suspension. After 2 h of stirring, the precipitate was filtered off and washed 4 times with water.

All catalysts were dried afterwards in a stream of air (363 K, 24 h). For calcination, the catalysts were heated up in an air stream from room temperature to 773 K in 4 h, this temperature was held for 2 h. The catalysts were reduced in a hydrogen stream, the temperature was programmed from room temperature to 773 K in 2 h and held at this temperature for 2 h.

The ruthenium catalysts were prepared by precipitation using $RuCl_3$ and by impregnation using $Ru(acac)_3$ as precursor. For precipitation, the calculated amount of $RuCl_3$ was dissolved in distilled water (approx. 100 mL per g $RuCl_3$). The support was filled in a 1 L round-bottom flask and suspended in water until stirring was possible. The $RuCl_3$ solution was added and stirred for 1 h. The slurry was heated (353 K) and 5 N NH_4OH solution (3 mL per g $RuCl_3$) was added through a dropping funnel. The catalyst was filtered off and dried in an oven (393 K). Calcination was carried out in flowing air (473 K, 3 h), reduction in a hydrogen flow (573 K, 3 h).

The catalyst Ru05Ai was prepared as follows: the support (73 g) was suspended in toluene (150 mL) and stirred for 15 min by a magnetic stirrer. Ruthenium acetylacetonate (2.907 g) was dissolved in toluene (150 mL) and the solution was added to the slurry of the support. The slurry was stirred for 1 h and the toluene was allowed to evaporate at room temperature. From time to time, the slurry was swirled to homogenise it. The catalyst was heated in a stream of helium within 4 h to 250 °C, this temperature was held for 2 h. For reduction, the catalyst was heated in a hydrogen stream within 1 h to 350 °C, the temperature was held for 3 h. The other ruthenium catalysts made by impregnation were synthesised by the same procedure using different supports and ruthenium loads. The catalysts are listed in Table 4.

The commercial nickel catalyst Ni68T (KataLeuna, Leuna, Germany) was used as delivered.

Characterisation of the Catalysts

The characterisation of the catalysts was done using the following techniques.

The metal contents of the catalysts were determined by atomic emission spectroscopy with inductively coupled plasma (ICP-OES, Perkin Elmer Optima 3000XL) after dissolving the materials in a mixture of HF/HNO_3 by means of an MDS-2000 microwave unit (CEM). The metal leaching was investigated by determining the metal content of the product solution in the same way. The solution was therefore in most cases also dissolved in a mixture of HF/HNO_3 using an MDS-2000 microwave unit (CEM).

Transmission electron microscopy (TEM) for qualitative and quantitative characterisation of the catalysts was carried out using a JEM 100C operating at 100 kV for transmission electron microscopy (TEM) in bright field and dark field modes. For electron microscopy examination the catalyst samples were dissolved in 2-propanol, dispersed carefully in an ultrasonic bath and then deposited on carbon-coated copper grids.

BET surface and BJH pore size were analysed on a Sorptomatic (Fisons) using nitrogen as adsorbent gas. The average load was 200 mg catalyst. The isotherms were evaluated with WinADP (CE Instruments). Standard isotherm for the BJH analyses was hydroxylated silica. BET calculations were performed between $p/p_0 = 0-0.4$, BJH calculations between $p/p_0 = 0.001-1$. One sample (Ni20Org1) was analysed also on an ASAP 2010 (Micromeretics) to confirm the results from the Sorptomatic.

XRF analyses were performed on a SPECTRO X-Lab (SPECTRO Analytical instruments, Kleve). Targets were HOPG for the range between 0 and 12 keV and Al_2O_3 for the range between 0 and 50 keV.

Hydrogenation of Glucose

The discontinuous hydrogenation was performed in an 300 mL autoclave (Parr Instruments) at the following conditions: temperature $T = 393$ K, total pressure $p = 120$ bar, glucose concentration: 40 wt % glucose in aqueous solution (120 mL), reaction time $t = 5$ h, stirring at 850 rpm. The catalysts were ground to < 63 μm, 0.5 g were used for the experiments. The apparatus was equipped with a mass flow controller to deliver in addition the amount of hydrogen which was converted during reaction to carry the reaction out at constant pressure. The product distribution was analysed by HPLC/RID detection (column: Aminex HPX-87C operated at 80 °C, eluent water, 0.6 mL/min.). Gluconic acid was determined by HPLC using an Aminex HPX 87H column operated at 45 °C with 0.6 mL/min. 0.0005 M H_2SO_4 as eluent, detectors were RID and DAD.

Continuous hydrogenation was performed in a trickle bed reactor (Catatest, Vinci Technologies, France). The glucose solution was stored under helium pressure in the feed vessel and delivered by an HPLC pump to the reactor. Hydrogen was delivered by a mass flow controller. Both flowed downstream through the reactor. The reactor was packed with the catalyst between two plugs of glass wool. Having passed the reactor the product solution flowed through a heat exchanger to the gas-liquid separator. Gas and product flows were depressurised to 10 bar. An effluent weir controlled the hydrogen effluent to maintain system pressure, another directed the liquid to the product vessel. Standard reaction conditions were: feed 40 mL/h 40 wt % glucose in distilled water degassed under vacuum (15 min), 23 L/h hydrogen, pressure of 80 bar, 40 mL of catalyst, 373 K reactor temperature. The catalyst pellets were ground and sieved, the fraction between 0.8 and 1.2 mm was used for filling the reactor. The catalysts were reduced with a hydrogen flow (40 L/h) under atmospheric pressure (2 h, 473 K). Afterwards they were rinsed with deionised water under standard conditions until no further particles were registered in the effluent. The reaction products were analysed as indicated before. Some samples were analysed for gluconic acid.

Acknowledgements

The authors thank the Federal Ministry of Research and Education (BMBF, Germany) for financial support (contract 03C0290C). Further we thank Dr. C. Mohr for TEM analyses, Dr. R. Schödel, KataLeuna for XRD, TPR and chemisorption analyses, Dr. M. Heck, TU Darmstadt for XRF analyses.

References

[1] H. Li, H. Li, J.-F. Deng, *Catal. Today* **2002**, *74*, 53 – 63.
[2] H. Li, W. Wang, J.-F. Deng, *J. Catal.* **2000**, *191*, 257 – 260.
[3] P. Gallezot, P. J. Cerino, B. Blanc, G. Flèche, P. Fuertes, *J. Catal.* **1994**, *146*, 93 – 102.
[4] N. Déchamp, A. Gamez, A. Perrand, P. Gallezot, *Catal. Today* **1995**, *24*, 29 – 35.
[5] J. Wisniak, R. Simon, *Ind. Eng. Chem. Prod. Res. Dev.* **1979**, *18*, 50 – 57.
[6] J. Wisniak, M. Heshkowitz, S. Stein, *Ind. Eng. Chem. Prod. Res. Dev.* **1974**, *13*, 232.
[7] K. van Gorp, E. Boerman, C. V. Cavenaghi, P. H. Berben, *Catal. Today* **1999**, *52*, 349 – 361.
[8] A. W. Heinen, J. A. Peters, H. van Bekkum, *Carbohydr. Res.* **2000**, *328*, 449 – 457.
[9] B. J. Arena, *Appl. Catal. A* **1992**, *87*, 219 – 229..
[10] P. Gallezot, N. Nicolaus, G. Flèche, P. Fuertes, A. Perrand, *J. Catal.* **1998**, *180*, 51 – 55.
[11] R. Liedke, *PhD thesis*, Universität Münster, Germany, **1999**.
[12] M. Makkee, P. G. Kieboom, H. van Bekkum, *Carbohydr. Res.* **1985**, *138*, 225 – 236.
[13] C. T. Kresge, M. E. Leonovicz, W. J. Roth, J. C. Vartuli, J. S. Beck, *Nature* **1992**, *359*, 710 – 712.
[14] S. Valange, J. Barrault, A. Derouault, Z. Gabelica, *Micropor. Mesopor. Mater.* **2001**, *44 – 45*, 211 – 220.
[15] Z. X. Cheng, C. Louis, M. Che, *Stud. Surf. Sci.*; **1995**, *91*, 1027 – 1036.
[16] S. Schimpf, C. Louis, P. Claus, in preparation.

CORRIGENDUM

In the paper by Burkhard Kusserow, Sabine Schimpf and Peter Claus in Issue 1 + 2, 2003, pp. 289 – 299, the reaction temperature given in the text on p. 295, first line of the right column, should read 373 K and not 353 K. The value given in the experimental section on p. 299 is correct. The authors apologize for this error.